Magnetic and electric excitations in split ring resonators

Jiangfeng Zhou[1,2,*], **Thomas Koschny**[1,3] **and Costas M. Soukoulis**[1,3]

[1]*Ames Laboratory and Department of Physics and Astronomy,Iowa State University, Ames, Iowa 50011*

[2]*Department of Electrical and Computer Engineering and Microelectronics Research Center, Iowa State University, Ames, Iowa 50011*

[3]*Institute of Electronic Structure and Laser - FORTH,and Department of Materials Science and Technology, University of Crete, Greece*

[*] *jfengz@iastate.edu*

Abstract: We studied the electric and magnetic resonances of U-shaped SRRs. We showed that higher order excitation modes exist in both of the electric and magnetic resonances. The nodes in the current distribution were found for all the resonance modes. It turns out that the magnetic resonances are the modes with odd-number of half-wavelength of the current wave, i.e. $\lambda/2$, $3\lambda/2$ and $5\lambda/2$ modes, and the electric resonances are modes with integer number of whole-wavelength of current wave, i.e. λ, 2λ and 3λ modes. We discussed the electric moment and magnetic moment of the electric and magnetic resonances, and their dependence to the length of two parallel side arms. We show that the magnetic moment of magnetic resonance vanishes as the length of side arms of the SRR reduces to zero, i.e. a rod does not give any magnetic moment or magnetic resonance.

OCIS codes: (160.3918) Metamaterials; (350.3618) Left-handed materials; (160.4760) Optical properties; (260.5740) Resonance.

References and links

1. V. G. Veselago, "Experimental demonstration of negative index of refraction," Sov. Phys. Usp. **10**, 509 (1968).
2. D. R. Smith, J. B. Pendry, and M. C. K. Wiltshire, "Metamaterials and negative refractive index," Science **305**(5685), 788–792 (2004).
3. C. M. Soukoulis, M. Kafesaki, and E. N. Economou, "Negative-index materials: New frontiers in optics," Advanced Materials **18**, 1941–1952 (2006).
4. S. Linden, C. Enkrich, G. Dolling, M. W. Klein, J. F. Zhou, T. Koschny, C. M. Soukoulis, S. Burger, F. Schmidt, and M. Wegener, "Photonic metamaterials: Magnetism at optical frequencies," IEEE Journal of Selected Topics in Quantum Electronics **12**, 1097–1105 (2006).
5. V. M. Shalaev, "Optical negative-index metamaterials," Nature Photonics **1**(1), 41–48 (2007).
6. C. M. Soukoulis, S. Linden, and M. Wegener, "Negative refractive index at optical wavelengths," Science **315**(5808), 47–49 (2007).
7. R. S. Penciu, M. Kafesaki, T. F. Gundogdu, E. N. Economou, and C. M. Soukoulis, "Theoretical study of left-handed behavior of composite metamaterials," Photonics Nanostructures-fundamentals Applications **4**(1), 12–16 (2006).
8. N. Katsarakis, M. Kafesaki, I. Tsiapa, E. N. Economou, and C. M. Soukoulis, "High transmittance left-handed materials involving symmetric split-ring resonators," Photon. and Nanostruct.: Fundam. and Appl. **5**, 149 (2007).
9. J. Pendry, A. Holden, D. Robbins, and W. Stewart, "Magnetism from Conductors and Enhanced Nonlinear Phenomena," IEEE Trans. Microwave Theroy Tech. **47**, 2075 (1999).

#88148 - $15.00 USD Received 3 Oct 2007; revised 16 Nov 2007; accepted 19 Nov 2007; published 14 Dec 2007

10. D. Smith, W. Padilla, D. Vier, S. Nemat-Nasser, and S. Schultz, "Composite medium with simultaneously negative permeability and permittivity," Physical Review Letters **84**, 4184 (2000).
11. T. J. Yen, W. J. Padilla, N. Fang, D. C. Vier, D. R. Smith, J. B. Pendry, D. N. Basov, and X. Zhang, "Terahertz magnetic response from artificial materials," Science **303**, 1494–1496 (2004).
12. S. Linden, C. Enkrich, M. Wegener, J. F. Zhou, T. Koschny, and C. M. Soukoulis, "Magnetic response of metamaterials at 100 terahertz," Science **306**, 1351–1353 (2004).
13. C. Enkrich, M. Wegener, S. Linden, S. Burger, L. Zschiedrich, F. Schmidt, J. F. Zhou, T. Koschny, and C. M. Soukoulis, "Magnetic Metamaterials at Telecommunication and Visible Frequencies," Physical Review Letters **95**(20), 203901 (pages 4) (2005). URL http://link.aps.org/abstract/PRL/v95/e203901.
14. N. Katsarakis, G. Konstantinidis, A. Kostopoulos, R. Penciu, T. Gundogdu, M. Kafesaki, E. Economou, T. Koschny, and C. M. Soukoulis, "Magnetic response of split-ring resonators in the far-infrared frequency regime," Optics Letters **30**, 1348–1350 (2005).
15. N. Katsarakis, T. Koschny, M. Kafesaki, E. N. Economou, and C. M. Soukoulis, "Electric coupling to the magnetic resonance of split ring resonators," Applied Physics Letters **84**(15), 2943–2945 (2004). URL http://link.aip.org/link/?APL/84/2943/1.
16. J. F. Zhou, L. Zhang, G. Tuttle, T. Koschny, and C. M. Soukoulis, "Negative index materials using simple short wire pairs," Physical Review B (Condensed Matter and Materials Physics) **73**(4), 041101 (pages 4) (2006). URL http://link.aps.org/abstract/PRB/v73/e041101.
17. J. F. Zhou, T. Koschny, L. Zhang, G. Tuttle, and C. M. Soukoulis, "Experimental demonstration of negative index of refraction," Applied Physics Letters **88**(22), 221103 (pages 3) (2006). URL http://link.aip.org/link/?APL/88/221103/1.
18. S. Zhang, W. Fan, B. K. Minhas, A. Frauenglass, K. J. Malloy, and S. R. J. Brueck, "Midinfrared Resonant Magnetic Nanostructures Exhibiting a Negative Permeability," Physical Review Letters **94**(3), 037402 (pages 4) (2005). URL http://link.aps.org/abstract/PRL/v94/e037402.
19. S. Zhang, W. Fan, N. C. Panoiu, K. J. Malloy, R. M. Osgood, and S. R. J. Brueck, "Experimental Demonstration of Near-Infrared Negative-Index Metamaterials," Physical Review Letters **95**(13), 137404 (pages 4) (2005). URL http://link.aps.org/abstract/PRL/v95/e137404.
20. G. Dolling, C. Enkrich, M. Wegener, C. M. Soukoulis, and S. Linden, "Low-loss negative-index metamaterial at telecommunication wavelengths," Optics Letters **31**, 1800–1802 (2006).
21. G. Dolling, C. Enkrich, M. Wegener, C. M. Soukoulis, and S. Linden, "Simultaneous Negative Phase and Group Velocity of Light in a Metamaterial," Science **312**, 892 (2006).
22. G. Dolling, M. Wegener, C. M. Soukoulis, and S. Linden, "Negative-index metamaterial at 780 nm wavelength," Optics Letters **32**(1), 53–55 (2007).
23. U. K. Chettiar, A. V. Kildishev, H. K. Yuan, W. Cai, S. Xiao, V. P. Drachev, and V. M. Shalaev, "Dual-band negative index metamaterial: double negative at 813 nm and single negative at 772 nm," Optics Letters **32**, 1671–1673 (2007). URL http://www.opticsinfobase.org/abstract.cfm?URI=ol-32-12-1671.
24. D. R. Smith, S. Schultz, P. Markos, and C. M. Soukoulis, "Determination of effective permittivity and permeability of metamaterials from reflection and transmission coefficients," Physical Review B (Condensed Matter and Materials Physics) **65**(19), 195104 (pages 5) (2002). URL http://link.aps.org/abstract/PRB/v65/e195104.
25. D. R. Smith, D. C. Vier, T. Koschny, and C. M. Soukoulis, "Electromagnetic parameter retrieval from inhomogeneous metamaterials," Physical Review E **71**(3), 036,617 (2005).
26. T. Koschny, P. Markos, E. N. Economou, D. R. Smith, D. C. Vier, and C. M. Soukoulis, "Impact of inherent periodic structure on effective medium description of left-handed and related metamaterials," Physical Review B (Condensed Matter and Materials Physics) **71**(24), 245105 (pages 22) (2005). URL http://link.aps.org/abstract/PRB/v71/e245105.
27. T. Koschny, M. Kafesaki, E. N. Economou, and C. M. Soukoulis, "Effective medium theory of left-handed materials," Physical Review Letters **93**(10) (2004).
28. T. Koschny, P. Markos, D. R. Smith, and C. M. Soukoulis, "Resonant and antiresonant frequency dependence of the effective parameters of metamaterials," Physical Review E **68**(6), 065,602 (2003).
29. C. Rockstuhl, F. Lederer, C. Etrich, T. Zentgraf, J. Kuhl, and H. Giessen, "On the reinterpretation of resonances in split-ring-resonators at normal incidence," Optics Express **14**(19), 8827–8836 (2006).
30. C. Rockstuhl, T. Zentgraf, E. Pshenay-Severin, J. Petschulat, A. Chipouline, J. Kuhl, T. Pertsch, H. Giessen, and F. Lederer, "The origin of magnetic polarizability in metamaterials at optical frequencies - an electrodynamic approach," Optics Express **15**(14), 8871–8883 (2007).

1. Introduction

The idea of negative index materials (NIMs), i.e. materials with both negative electrical permittivity, ε, and magnetic permeability, μ, was first introduced by Veselago [1]. However, it was only recently that such materials were investigated experimentally[2, 3, 4, 5, 6, 7, 8]. Although it has been well known how to obtain $\varepsilon < 0$ material easily (e.g. using lattice of metallic wires),

#88148 - $15.00 USD Received 3 Oct 2007; revised 16 Nov 2007; accepted 19 Nov 2007; published 14 Dec 2007

the realization of $\mu < 0$ (especially at high frequencies) response had been a challenge, due to the absence of naturally occurring magnetic materials with negative μ. In 1999, Pendry et al. [9] suggested a design made a two concentric metallic rings with gaps, called split ring resonators (SRRs), which exhibit a $\mu < 0$ around the magnetic resonance frequency ω_m. Immediately after Smith et al. [10] fabricated the first negative index material at GHz frequencies. Recently different groups observed [11, 12, 13, 14] indirectly negative μ at THz frequencies. In most of the THz experiments, only one layer of SRRs were fabricated on a substrate and the transmission, T, was measured only for propagation perpendicular to the plane of the SRRs, exploiting the coupling of the electric field to the magnetic resonance of the SRR via asymmetry [15]. It was realized that one only need the single SRR to see the magnetic resonance effects. This way is not possible to drive the magnetic permeability negative. One reason is that is very difficult to measure with the existing topology of SRRs and continuous wires both the transmission, T, and reflection, R, along the direction parallel to the plane of the SRRs. So there is a need for alternative, improved and simplified designs that can be easily fabricated and experimentally characterized. This new design was recently achieved in the GHz region [16, 17] and the THz region [18, 19, 20, 21] by the use of finite length of wires and the fishnet topology. Very recent work has moved the negative refractive index into optical wavelength [22, 23].

In this manuscript we systematically studied the electric and the magnetic resonances response of U-shaped SRRs for different propagating directions. The effective electric permittivity, ε, as well as the magnetic permeability, μ will be extracted by the retrieval procedure [24, 25, 26]. In addition, the current distribution along the sides of the U-shaped SRR will be numerically calculated. We show that the magnetic resonances are modes with odd-number of half-wavelength of the current density wave, while the electric resonances are modes with integer number of whole-wavelength the current density wave. In addition we studied the dependence of the electric and magnetic resonances as a function of the length of the side arms of the U-shaped SRR. It is found that the magnetic moment of the U-shaped SRR vanishes as the length of side arms of SRR reduces to zero. So there is no magnetic moment or magnetic resonance for a metallic rod. One needs the side arms of the U-shaped SRR in order to have a magnetic moment.

2. Electric and magnetic responses of SRRs

A common constituent to provide magnetic response in metamaterials is the Split-Ring resonator (SRR). The SRR in its simplest form consists of a highly conductive metallic ring which is broken in one (or several) location(s) by a non-conductive gap of air or other dielectric materials. If this ring is placed in a temporally varying magnetic field an electric circular current is induced in the metallic ring which in turn leads to charge accumulating across the gaps. The electric field which builds due to the charge at the gap counteracts the circular current leading to energy stored (predominantly) in vicinity of the gaps and magnetic field energy concentrated in the region enclosed by the ring. The SRR is thus a resonator which couples to a perpendicular magnetic field and can be characterized by the effective capacitance of the gaps and effective inductance of the loop define by the ring. It can be understood in terms of a resonant LC circuit with a resonance frequency $\omega_m^2 = 1/LC$, where L is the inductance and C is the capacitance of the SRR. The resonant response of the circular current in the SRR to an external magnetic field leads to a resonant magnetic moment which may reach large negative values for array of SRRs such that the size of the SRR is much smaller than the wavelength of an incident electromagnetic wave around the resonance frequency behaves as a homogeneous effective medium with at negative (resonant) permittivity $\mu_{\text{eff}}(\omega)$.

In this letter we report numerical results of electric and magnetic responses of a periodic lattice of SRRs for different orientations of the SRRs with respect to the external electric field,

#88148 - $15.00 USD Received 3 Oct 2007; revised 16 Nov 2007; accepted 19 Nov 2007; published 14 Dec 2007

$\vec{E}$, and the direction of propagation, $\vec{k}$.

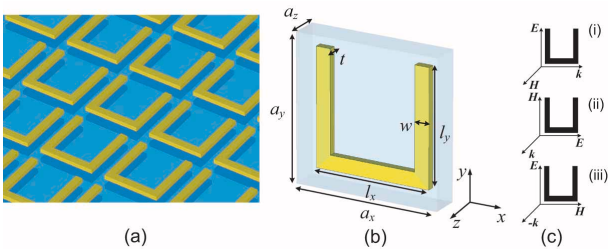

Fig. 1. (a) Schematic of periodically arranged U-shaped SRR arrays; (b) a single unit cell with geometrical parameters; (c) three different configurations of incident electric field, $\vec{E}$, magnetic field, $\vec{H}$, and wave vector, $\vec{k}$.

Our numerical simulations were done with CST Microwave Studio (Computer Simulation Technology GmbH, Darmstadt, Germany), which uses a finite-integration technique, and Comsol Multiphysics, which uses a frequency domain finite element method. The schematic of the periodic U-shaped SRRs arrays and the geometry of a single unit cell used in our numerical simulation were shown in Fig. 1(a) and 1(b), respectively. The SRRs exhibit different responses to the incident electromagnetic (EM) wave with respect to different configurations of incident electric field, $\vec{E}$, magnetic field, $\vec{H}$, and wave vector, k, as shown in Fig. 1(c). First, it is well known that the incident EM wave excites a magnetic resonance at ω_m [9, 2, 3, 4, 5, 6] if the external magnetic field, $\vec{H}$, is perpendicular to the SRR plane and the wave vector, $\vec{k}$, is parallel to the SRR plane (Fig. 1(c.i)). Second, farther study reveals that the incident EM wave with $\vec{k}$ perpendicular to the SRR plane and $\vec{E}$ parallel to the bottom part of SRR (Fig. 1(c.ii)) also excites a magnetic resonance at ω_m [15]. This magnetic resonance results from a circular current induced by the external electric field, $\vec{E}$, because of the asymmetry of the SRR in the direction of $\vec{E}$, and therefore was called the electric excitation coupling to the magnetic resonance (EEMR). The EEMR is very valuable for the experimental demonstration of the magnetic resonance at optical frequencies, because it is very difficult to measure the transmission and reflection with the incident EM wave parallel to the SRR plane at optical frequencies [11, 12, 13, 14, 15]. Third, the SRRs also exhibit a short-wire-like electric resonance [27] at ω_0 with the incident electric field, $\vec{E}$, parallel to the side part of SRRs (Fig. 1(c.iii)). The electric resonance frequency ω_0 depends on the length of the side part of SRRs, l_y, being higher for shorter l_y.

Using the retrieval procedure [24, 25, 26], we calculated the effective permittivity $\varepsilon(\omega)$ and permeability $\mu(\omega)$, both real and imaginary part, from the simulated transmission, T, and reflection, R. Fig. 2 shows the extracted real part of the effective permittivity $\mathrm{Re}(\varepsilon(\omega))$ and permeability $\mathrm{Re}(\mu(\omega))$ for three different polarized incident EM waves as shown in Fig. 1(c). As expected, the magnetic resonance, measured by μ (red solid)), occurs at around $\omega_m = 55$ THz. The EEMR gives a similar resonance at roughly the same frequency, shown as a resonance shape in ε (blue dashed), which indicate the response is due to the electric coupling of the incident EM wave to SRR. At a higher frequency, $\omega_0 = 135$ THz, the short-wire-like electric resonance of the SRR occurs, given by the resonance behavior of ε (green dotted). Due to the periodicity effect, whenever a magnetic resonance occurs in $\mathrm{Re}(\mu)$, an electric anti-resonance will be seen in $\mathrm{Re}(\varepsilon)$ simultaneously and vice versa [26, 28]. The periodicity effect becomes more noticeable as the wavelength of EM wave is comparable with the lattice constant of the SRR lattice. For the magnetic resonance (red solid), the lattice constant, $a_x = 1$ μm, in the propagating direction along the wave vector, $\vec{k}$, is comparable to the resonance wavelength, $\lambda_m = 5.45$ μm, hence, a strong distortion in the negative part of resonance in $\mathrm{Re}(\mu)$ and a sig-

#88148 - $15.00 USD Received 3 Oct 2007; revised 16 Nov 2007; accepted 19 Nov 2007; published 14 Dec 2007

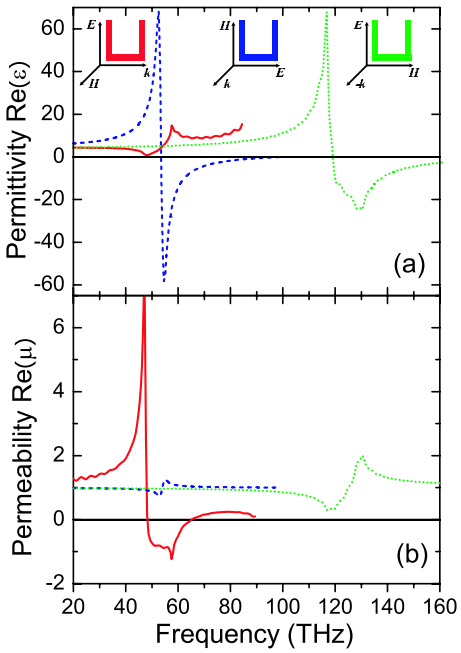

Fig. 2. Extracted effective permittivity $\mathrm{Re}(\varepsilon(\omega))$ (a) and effective permeability $\mathrm{Re}(\mu(\omega))$ (b) for the magnetic resonance (red solid), the electric excitation coupling to the magnetic resonance (EEMR) (blue dashed) and the short-wire-like resonance (green dotted) of U-shaped SRRs. The geometric parameters are $a_x = a_y = 1$ μm, $a_z = 0.2$ μm, $l_x = l_y = 0.8$ μm, $w = 0.1$ μm and $t = 0.05$ μm. The U-shaped SRR is made of gold described by the Drude model with plasma frequency, $f_p = 2175$ THz, and damping frequency, $f_\tau = 6.5$ THz.

nificant anti-resonance in $\mathrm{Re}(\varepsilon)$ were observed. On the other hand, for the EEMR, the lattice constant, $a_x = 0.2$ μm, is much smaller than λ_m, so the periodicity effect is much weaker and therefore a sharp resonance in $\mathrm{Re}(\varepsilon)$ (blue dashed) with a weak anti-resonance in $\mathrm{Re}(\mu)$ occurs.

3. Higher order excitation modes of SRRs

Beside the typical electric and magnetic response, the SRRs also exhibits higher order excitation modes. As shown in Fig. 3(a), for the incident EM wave with the propagating direction perpendicular to the plane of SRRs, we found three successive dips at 55 THz, 155 THz and 300 THz in the transmission spectra. Correspondingly, at the same frequencies, we found three resonance shapes in $\mathrm{Re}(\varepsilon)$ (Fig. 3(c)). The first excitation mode occurs at the lowest frequency $f_{m0} = 55$ THz, which is the usual EEMR response, and has the strongest resonance in $\mathrm{Re}(\varepsilon)$. The magnitudes of resonance of the second and third excitation modes, occur approximately at $3f_{m0}$ and $6f_{m0}$ respectively, and are much weaker then the first excitation mode. Higher order excitation modes of the short-wire-like response also been observed (Fig. 3(b) and 3(d)). In Fig. 3(b), four dips were found in the transmission spectra, which result from the first, second and third order electric excitation modes of SRRs. Detailed studies show that the second (205 THz) and the third (265 THz) dips in the transmission spectra have similar current density distribution, so they are both considered as the second excitation mode.

As a very crude picture we could imagine the resonances of the SRRs as charge density waves on a rod of a length equal to the arc length of the SRR ring. This rod supports plasmonic

#88148 - $15.00 USD Received 3 Oct 2007; revised 16 Nov 2007; accepted 19 Nov 2007; published 14 Dec 2007

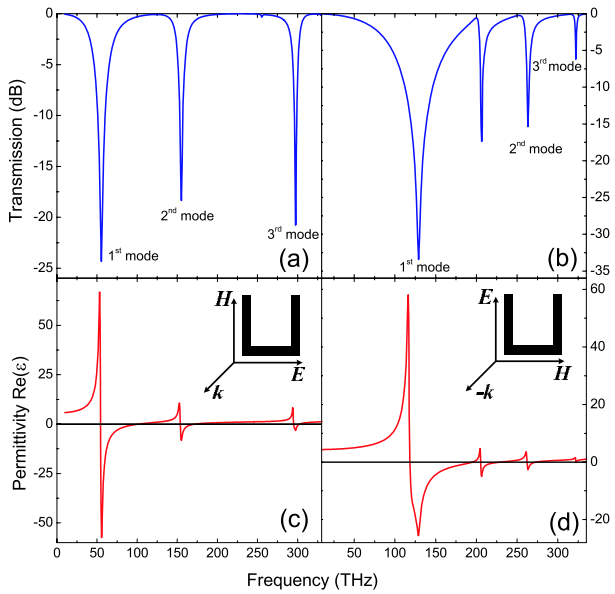

Fig. 3. Transmission spectra (a,b) and the extracted permittivity, Re(ε), (c,d) of the U-shaped SRRs response to the incident EM wave. The directions of $\vec{E}$, $\vec{H}$ and $\vec{k}$ were shown as the insets.

modes [29, 30] (plasmonic means in this situation that the inductance is coming from the electron mass and the capacitance from the external electric field over the surface of the rod) which occur at discrete frequencies whenever we have current nodes at the ends of the rod. This picture is of limited value for the following reasons: (i) the EM response of the modes, especially the classification of electric vs. magnetic response, depends on the geometry and is entirely different for a U-shaped SRR than for a straight rod although the qualitative current distribution over the arc length is equivalent; (ii) the plasmonic dispersion depends on the geometric inductance, i.e. the energy stored in the external field outside the metal, which is much larger for the SRR than for the rod and spatially non-uniform along the SRR ring; and (iii) the modes of coupling are different. Nevertheless, considering the current distribution is an essential tool for understanding the resonant modes of a SRR at higher THz frequencies. In the microwave region only the remnants of the lowest order mode survive.

Figure 4 shows the distribution of the current and charge density for the lowest three resonant modes of a U-shaped SRR of side length, $l_y = 800$ nm. The current density is obtained directly from the simulation results, the charge density relates to the perpendicular electric field at the surface of the metal. All fields are time harmonic; the current distributions are shown temporally $\pi/2$ phase shifted against the charge distribution. The first three panels (a,b,c) of Fig. 4 show the lowest three EEMR resonances for normal incidence to the SRR with the electric field breaking the symmetry of the SRR and thus we have coupling to the ”magnetic” resonance[15]. The surface electric field distribution is qualitatively equivalent to the pure magnetic coupling (i.e. propagation in the SRR plane with perpendicular magnetic field), which case is however hard to realize experimentally at such high THz frequencies. All three modes have non-zero magnetic moment coming from all three ”arms” of the SRR. The number of current nodes (where charge accumulates) increases with the resonance frequency from two (fundamental mode, corresponding to the resonance of the effective *LC* circuit), one on either side of the ”gap”, to four and six, which have additional nodes inside the continuous metal. The electric

#88148 - $15.00 USD Received 3 Oct 2007; revised 16 Nov 2007; accepted 19 Nov 2007; published 14 Dec 2007

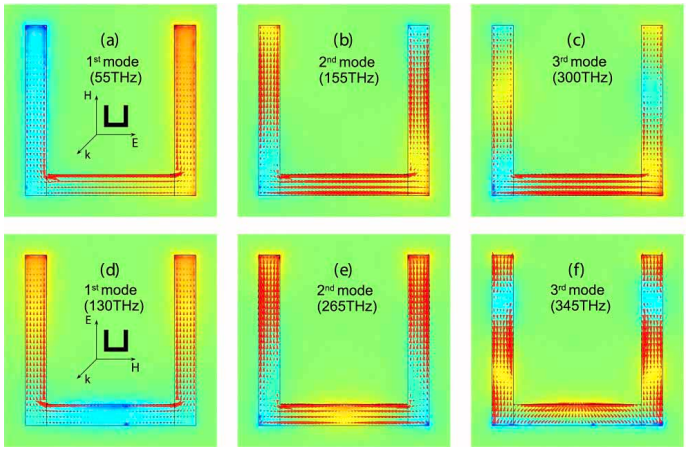

Fig. 4. Distribution of the perpendicular component of the surface electric field (color scale; red positive, blue negative) and the bulk current density (arrows) for the lowest few resonant modes of the SRR. The SRR metal is made of a Drude model for gold ($f_p = 2175$ THz, $f_\tau = 6.5$ THz), the geometry parameters are: $a_x = a_y = 1$ μm, $a_z = 200$ nm (unit cell size), $l_x = l_y = 800$ nm (arm length), $w = 100$ nm, $t = 50$ nm (ring width and thickness, respectively). The current distributions are shown temporally $\pi/2$ phase shifted against the charge distribution.

excitation of these modes occurs via the polarization of the bottom arm of the SRR by the electric field of the incident EM wave. For a straight rod, these SRR modes would correspond to the $\lambda/2$, $3\lambda/2$, and $5\lambda/2$ mode (Fig. 5(a)); however, for the metallic rod, there is no magnetic moment associated with the excitation modes. Note that these modes also possess an electric dipole moment; therefore the SRR has a combined magnetic and electric response in this configuration. For the other polarization, normal incidence to the SRR with the electric field along the symmetry axis of the SRR, shown in panels (d,e,f) of Fig. 4, we see the analog plasmonic modes with three, five and seven current nodes; all of which reflect the mirror symmetry of the SRR and can thus have no magnetic moment. For the metallic rod, they would correspond to the even, λ, 2λ, and 3λ modes (which cannot be exited for the rod because of their vanishing dipole moment). In the case of the SRR they do possess electric dipole moment in the **E**-direction, i.e. along the two parallel arms of the SRR, and represent a purely electric response of the SRR.

Figure 5(a) and 5(b) show the distribution of the total current (current density **j** integrated over the cross-section of the SRR ring) over the arc length around the SRR ring for the three resonant modes of Fig. 4(a,b,c) and Fig. 4(d,e,f) respectively. We clearly see the different number of current nodes, which do not reach zero (for the higher modes) because of the superposition with the non-resonant response of the lower order modes (which are fairly broad due to the high losses). Also note the non-uniform spacing of the nodes for the higher orders which are different from the straight rod and are due to the curvature of the SRR and the coupling to the bottom arm or side arms only.

4. Electric and magnetic moments of SRRs

We also studied the electric moment and the magnetic moment for the electric excitation of the magnetic resonance (EEMR) and the short-wire-like resonance of the U-shaped SRRs with different length of two parallel side arms, l_y. The electric moment is calculated by the integration

#88148 - $15.00 USD Received 3 Oct 2007; revised 16 Nov 2007; accepted 19 Nov 2007; published 14 Dec 2007

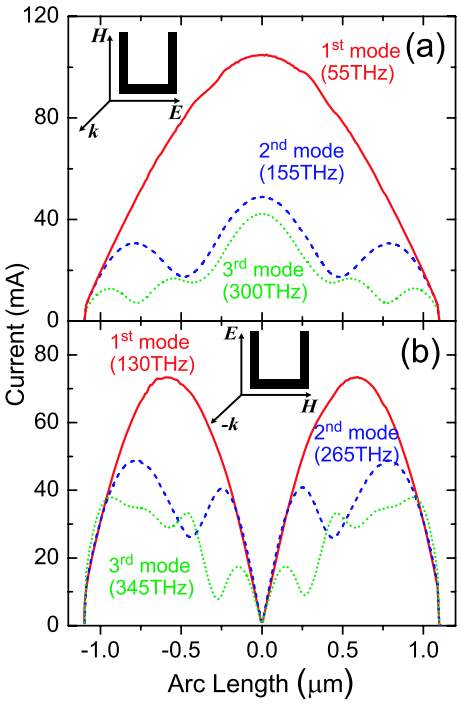

Fig. 5. Current distribution of the lowest 3 modes. (a) $\lambda/2$, $3\lambda/2$, and $5\lambda/2$ mode for the EEMR response; (b) λ, 2λ, and 3λ mode for the short-wire-like response. Due to the nonzero response of lower order modes, nodes of higher order modes only reach zero at the positions of the lowest nodes.

of the subtraction between the electric displacement $\vec{D}$ and vacuum electric displacement $\varepsilon_0\vec{E}$ over the volume of the whole unit cells.

$$\vec{p} = \int (\vec{D} - \varepsilon_0\vec{E})\mathrm{d}\vec{r}$$

Then the electric polarization, normalized by incident electric field, $\mathbf{E_0}$, $\vec{P} = \vec{p}/(VE_0)$ is shown in Fig. 6(a) and 6(b) for the EEMR and the short-wire-like response of the SRRs respectively. It is clearly seen that the lowest mode of the resonance has the strongest electric moment although the higher order excitation also has nonzero value. In Fig. 6(a), the electric polarization, P_x, decreases as the length of two parallel arms, l_y, decreases, because the EEMR response becomes weaker and finally disappeared as the length l_y close to zero (green dotted curve). However, the electric polarization, P_x, does not vanish in the limiting case of $l_y = 0$, (green dotted curve), because the EEMR degenerates to the short-wire-like electric resonance of the bottom arm of the SRR which results in the non-zero electric polarization. The polarization density along the y-direction, P_y, of the short-wire-like resonance of the SRR (Fig. 6(b)) with the incident electric field $\vec{E}$ parallel to the side arms of the SRR, also decreases and shifts to higher frequencies as l_y decreases.

The magnetic moment is calculated by employing the formula:

$$\vec{m} = \frac{j\omega}{2}\int \vec{r}\times(\vec{D} - \varepsilon_0\vec{E})\mathrm{d}\vec{r}$$

In Fig. 7(a), we show the magnetic moment, normalized by the magnetic field of the inci-

#88148 - $15.00 USD Received 3 Oct 2007; revised 16 Nov 2007; accepted 19 Nov 2007; published 14 Dec 2007

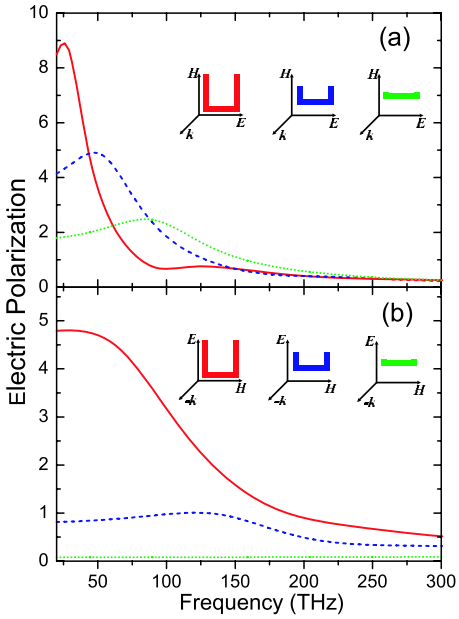

Fig. 6. Magnitude of the normalized polarization density, P, of the U-shaped SRRs with $l_y = 0.8\ \mu$m (red solid), 0.4 μm (blue dashed) and 0.11 μm (green dotted), respectively. (a) P_x component as $\vec{E}$ parallel to the bottom part of SRRs. The other two components P_y and P_z are nearly zero (not shown in the figure); (b) P_y component as $\vec{E}$ parallel to the side part of SRRs. The other two components P_x and P_z are nearly zero (not shown in the figure). The polarizations of the incident EM wave are shown as the insets in the panel (a) and (b). The x, y and z coordinates were shown in Fig. 1.

dent EM wave, $\mathbf{H_0}$, $\vec{M}_z = \vec{m}_z/(VH_0)$, and in Fig. 7(b), the extracted permittivity, Re(ε), for the magnetic resonant modes of the SRR as a function of frequency for three different U-shaped SRRs with different lengths of the two parallel arms, l_y. It is clearly seen that the lowest order magnetic resonance provides the strongest magnetic response; but also the higher modes have non-zero magnetic moment. As we expect, the magnetic moment decreases as the length of the side arm of SRRs , l_y, decreases, and at the same time, the magnetic resonance shifts to higher frequency. This is a combined effect of shortened arc length and reduced the geometric loop inductance. In the limit of $l_y = 0$, only the bottom arm left (i.e. a straight rod), the magnetic response would vanish (green dotted curve), and no magnetic response is seen, as expected. In this limiting case, the resonance in Re(ε) still exists, which is a result from the electric resonance of the bottom arm of SRR. Note that the magnitude of the resonance in Re(ε) decreases much slower than the magnetic moment does as the arm length, l_y, decreases. The reason is that the magnetic moment, m_z, resulting from the circular current flowing in the loops of the SRR, vanishes immediately as the side arms disappear, but the resonance in Re(ε) always exist as long as the short-wire-like electric resonance exists in the bottom part of the SRR. However, as shown in the green curve of Fig. 7(a), this short-wire-like electric resonance can not provide any magnetic moment.

The short-wire-like resonance with the propagating direction of the incident EM wave perpendicular to the SRR plane and the electric field, **E**, parallel to the side arms of the SRR (Fig. 1(c.iii)), has zero magnetic moment.

#88148 - $15.00 USD Received 3 Oct 2007; revised 16 Nov 2007; accepted 19 Nov 2007; published 14 Dec 2007

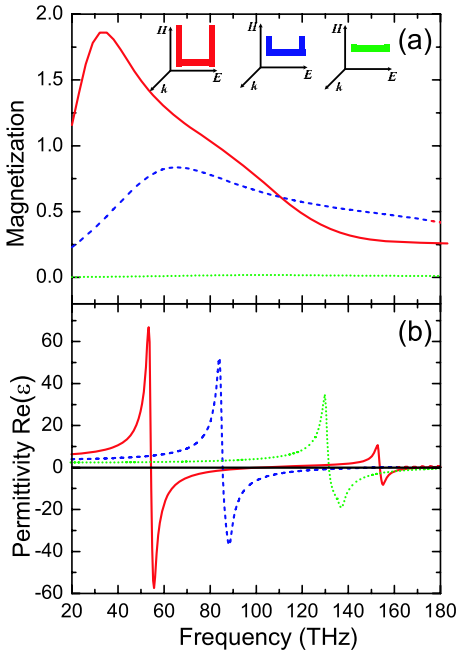

Fig. 7. (a) Magnitude of the normalized magnetization, M_z, and (b) the extracted permittivity, Re(ε), of the U-shaped SRRs with the length $l_y = 0.8$ μm (red solid), 0.4 μm (blue dashed) and 0.11 μm (green dotted), respectively. The polarizations of the incident EM wave are shown as the insets in the panel (a). The short-wire-like resonance with incident EM wave polarized as shown in Fig. 1(c.ii) has zero magnetic moment (not shown in the figure).

5. Conclusions

We systematically studied the electric and magnetic resonances of U-shaped SRRs with respective to different polarizations of the incident EM wave. Higher order excitation modes were found in both electric and magnetic resonances. We show that the magnetic resonances are the modes with odd-number of half-wavelength of the current density wave, while the electric resonances are modes with integer number of whole-wavelength of the current density wave. In addition, the current density distribution of the lowest three excitation modes was given. We also studied the magnetization density as a function of the length of the side arms of the U-shaped SRRs. It turns out that the magnetic resonance vanishes as the length of side arms reduces to zero, i.e. a rod does not give any magnetic moment or magnetic resonance.

Acknowledgments

Work at Ames Laboratory was supported by Dept. of Energy (Basic Energy Sciences) under contract No. DE-AC02-07CH11358, by the AFOSR under MURI grant (FA9550-06-1-0337), by Dept. of Navy, office of Naval Research (Award No. N0014-07-1-0359), EU FET projects Metamorphose and PHOREMOST, and by Greek Ministry of Education Pythagoras project.

#88148 - $15.00 USD Received 3 Oct 2007; revised 16 Nov 2007; accepted 19 Nov 2007; published 14 Dec 2007